

ResMem: Learn what you can and memorize the rest

Zitong Yang^{◇*}

zitong@berkeley.edu

[◇]Department of Statistics, Stanford University

Michal Lukasik[†] Vaishnavh Nagarajan[†] Zonglin Li[†] Ankit Singh Rawat[†]

Manzil Zaheer[†] Aditya Krishna Menon[†] Sanjiv Kumar[†]

{mlukasik, vaishnavh, lizonglin, ankitsrawat,
manzilzaheer, adityakmenon, sanjivk}@google.com

[†]Google Research, New York

Abstract

The impressive generalization performance of modern neural networks is attributed in part to their ability to *implicitly* memorize complex training patterns. Inspired by this, we explore a novel mechanism to improve model generalization via *explicit* memorization. Specifically, we propose the *residual-memorization* (*ResMem*) algorithm, a new method that augments an existing prediction model (e.g. a neural network) by fitting the model’s residuals with a k -nearest neighbor based regressor. The final prediction is then the sum of the original model and the fitted residual regressor. By construction, ResMem can explicitly memorize the training labels. Empirically, we show that ResMem consistently improves the test set generalization of the original prediction model across various standard vision and natural language processing benchmarks. Theoretically, we formulate a stylized linear regression problem and rigorously show that ResMem results in a more favorable test risk over the base predictor.

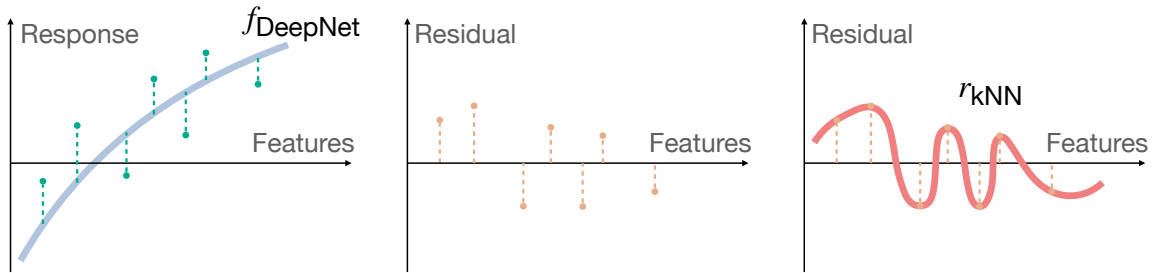
1 Introduction

Large neural networks achieve remarkable *generalization* on test samples despite *memorization* (achieving zero training error) of training samples [Zhang et al., 2017]. Several recent analyses have established that, under certain settings, memorization is *sufficient* to achieve generalization [Bartlett et al., 2017, Dziugaite and Roy, 2017, Belkin et al., 2018, Neyshabur et al., 2019, Bartlett et al., 2020], and, more surprisingly, can even be *necessary* [Feldman, 2020, Feldman and Zhang, 2020b, Cheng et al., 2022].

The above suggests that suitable memorization can be a valuable desiderata for learning. While increasing model size is a conceptually simple strategy to enable memorization, this has the obvious downside of significantly increasing the cost of model training and serving. This raises a natural question: are there alternate mechanisms to improve the memorization (and thus generalization) of a relatively small model?

In this paper, we propose *residual memorization* (*ResMem*), a simple yet effective mechanism that achieves this goal (Section 3). Compared to the *implicit* memorization performed by large neural models, the key idea of ResMem is to perform *explicit* memorization via a separate k -nearest neighbor component. Specifically, ResMem involves first training a standard neural network f_{DeepNet} , and then explicitly *memorizing the model’s residuals* with a k -nearest neighbor based regressor $r_{k\text{NN}}$ (cf. Figure 1). Memorization through k -nearest neighbor can be efficiently

*Work partly done at Google Research, New York.



(a) **Step 1:** learn the training set. (b) **Step 2:** compute the residual. (c) **Step 3:** memorize the residual.

Figure 1: Illustration of the *residual memorization* (ResMem) algorithm. In a nutshell, we first fit a small deep network f_{DeepNet} on the training sample (Figure 1(a)). When this network is non-memorizing, it incurs non-zero *residual* errors in its predictions (Figure 1(b)). We then fit a k -nearest neighbor based regressor on these residuals (Figure 1(c)). The final prediction is given by the sum of the initial network and k -NN regressor predictions. In all three figures, the x -axis represents the features in a supervised learning problem. In Figure 1(a), the y -axis represents the targets of prediction. In Figure 1(b) and 1(c), the y -axis represents the residual of the initial fitting from **Step 1**.

computed with various approximation schemes (e.g. Guo et al. [2020]). Subsequently, the ResMem prediction on an instance x is given by the sum of the two components, i.e., $f_{\text{DeepNet}}(x) + r_{\text{kNN}}(x)$.

We establish the efficacy of ResMem both theoretically and empirically, particularly when implicit memorization is infeasible, e.g., when the training set size is very large, or when the data patterns are too complex to learn perfectly. In Section 4, we show that ResMem consistently improves test accuracy (compared to a baseline DeepNet) on image classification tasks with ImageNet [Russakovsky et al., 2015] and CIFAR100 [Krizhevsky, 2009], and autoregressive language modeling on C4 [Raffel et al., 2020].

Towards understanding this improved performance, we hypothesize that ResMem works by learning in two-stages (cf. Section 4.2). Specifically, we posit that the initial DeepNet f_{DeepNet} learns some *coarse* structure, and ResMem r_{kNN} supplements the DeepNet prediction with *fine-grained* details (cf. Figure 2). We verify our hypothesis via qualitative analysis on CIFAR100 and C4 (Section 4.2).

To formalize the efficacy of ResMem, we formulate and analyze a stylized high dimensional linear regression problem that captures the essence behind ResMem (cf. Section 5). Our analysis (Theorem 5.3) shows that as the number of samples goes to infinity, the test risk of the base predictor decreases to an irreducible constant, whereas the risk of ResMem decreases to zero.

To summarize, our contributions are:

1. We propose *residual-memorization* (*ResMem*), a two-stage learning algorithm that combines a base prediction model with a nearest neighbor regressor (cf. Section 3);
2. We empirically demonstrate that ResMem improves test performance of neural networks (cf. Section 4), particularly when the training set is extremely large (cf. Section 4.3);
3. We theoretically analyze the rate of convergence of ResMem on a stylized linear regression problem, and show that it can improve upon the base prediction model (Section 5).

2 Background and Notation

In this section, we fix notation and discuss the relevant literature that motivates us to propose the ResMem algorithm.

2.1 Notation

We consider multi-class classification problems over instances \mathcal{X} and labels $\mathcal{Y} \doteq \{1, 2, \dots, L\} = [L]$. Given training examples $S = \{(x_i, y_i)\}_{i \in [n]} \in (\mathcal{X} \times \mathcal{Y})^n$, the goal is to learn a scorer $f: \mathcal{X} \rightarrow \mathbb{R}^L$ that, given an instance, assigns an affinity score for each label. Such an f should minimize the *misclassification error* on test samples:

$$L_{01}(f) \doteq \mathbb{P}_{(x,y)}(y \neq \text{pred}(f(x))), \quad (1)$$

where $\text{pred}(z) \doteq \arg \max_{y' \in [L]} z_{y'}$, and \mathbb{P} is the distribution over labelled instances. To achieve this, one typically minimizes the *empirical loss*

$$\hat{L}_\ell(f) \doteq \frac{1}{n} \sum_{i \in [n]} \ell(y_i, f(x_i)),$$

where $\ell: [L] \times \mathbb{R}^L \rightarrow \mathbb{R}_+$ is a loss function. Ideally, one would like to use $\ell_{01}(y, f(x)) \doteq 1(y \neq \text{pred}(f(x)))$; for computational tractability, it is popular to instead use a *surrogate loss*, such as the softmax cross-entropy:

$$\ell(y, f(x)) = -\log \frac{\exp(f_y(x))}{\sum_{y' \in [L]} \exp(f_{y'}(x))}.$$

2.2 Memorization for generalization: prior work

Memorization is sufficient for generalization. Overparameterised neural models with many more parameters than training samples have the capacity to perfectly fit (or *interpolate*) even random training labels [Zhang et al., 2017]; i.e., they can drive the empirical loss $\hat{L}_\ell(f) \rightarrow 0$ for *any* training set. At the same time, when trained on real-world datasets, increasing model complexity tends to *improve* model performance [Neyshabur et al., 2019, Yang et al., 2020]; that is, the models do not simply memorize the training sample, but rather learn generalizable patterns.

Several works have sought to understand the reasons behind this behaviour, both empirically [Arpit et al., 2017] and theoretically [Bartlett et al., 2017, Dziugaite and Roy, 2017, Brutzkus et al., 2018, Belkin et al., 2018, Neyshabur et al., 2019, Liang and Rakhlin, 2020, Montanari and Zhong, 2020, Bartlett et al., 2020, Vapnik and Izmailov, 2021, Wang et al., 2021, Yang et al., 2021]. One recurring message from the theory is that memorization (in the form of interpolation) can be sufficient for generalization.

Memorization can be necessary for generalization. Some recent works [Feldman, 2020, Cheng et al., 2022] showed that memorization — either in the sense of interpolation, or in a more general sense of stability [Feldman and Zhang, 2020a] — may be necessary for generalization. Feldman [2019] considered a setting where the label distribution exhibits a *long-tailed* distribution, and showed that to prevent incurring a large error on the large number of under-represented classes, it may be necessary to memorize many of their associated training samples. Cheng et al. [2022] considered a linear regression setting where it is beneficial to fit the training targets to error lower than the Bayes-error (i.e., the inherent noise in the targets).

3 Our method: ResMem

Prior works suggests that *implicit* memorization through increase in model size leads to better generalization. When such implicit memorization is infeasible — e.g., because of the increased computational cost of using a large model — is it possible to perform *explicit* memorization and get generalization benefits?

This motivates us to the propose the ResMem algorithm (c.f. Figure 1), which operates as follows:

ResMem — Residual Memorization

1. **Train the base DeepNet.** Train a neural network f_{DeepNet} on the training samples S as usual.
2. **Prepare the residual data.** Compute the *residual*^a prediction of each training example as

$$r_i = \text{onehot}(y_i) - \text{softmax}(f_{\text{DeepNet}}(x_i)/T), \quad \forall i \in [n],$$

where $\text{onehot}: \mathcal{Y} \rightarrow \mathbb{R}^L$ is the standard encoding that maps the label to a probability vector. Here, T is a hyperparameter corresponding to the “temperature” scaling of the softmax operation. Then, we employ the output of an intermediate layer of the base network f_{DeepNet} , denoted by $z_i = \phi(x_i)$, as an embedding for the training instance x_i . These embeddings are utilized for the nearest neighbor search in the next step.

3. **Predict via memorized residuals.** To make a prediction on a test sample $\tilde{x} \in \mathcal{X}$, first compute its embedding $\tilde{z} = \phi(\tilde{x})$. Then, use soft k -nearest neighbor method to build a function r_{kNN} defined by weights $\bar{w}_i(\tilde{x})$:

$$r_{\text{kNN}}(\tilde{x}) = \sum_{i=1}^n \bar{w}_i(\tilde{x}) \cdot r_i. \quad (2)$$

The weights $\bar{w}_i(\tilde{x})$ satisfy $\sum_i \bar{w}_i(\tilde{x}) = 1$, and are computed from raw weights w_i as follows:

$$w_i = \exp(-\|\tilde{z} - z_i\|_2/\sigma), \quad \bar{w}_i(\tilde{x}) \propto \mathbf{1}(w_i \geq w_{(k)}) w_i.$$

Here $w_{(k)}$ represents the k -th largest entry of w_i 's, and k, σ are two hyperparameters that collectively controls the locality of nearest neighbor search.

We make the final prediction based on the following scorer:

$$f_{\text{ResMem}}(\tilde{x}) = \text{softmax}(f_{\text{DeepNet}}(\tilde{x})/T) + r_{\text{kNN}}(\tilde{x}). \quad (3)$$

^aFor an overparameterized network that perfectly fits the training sample, the residuals will all be 0. However, we are interested in employing smaller networks, which will likely have non-zero residuals.

Remark 3.1 (Classification versus regression). The above introduces ResMem in a classification setting, which serves as our primary focus in the experiments in Section 4. That said, we

emphasize that ResMem can easily be extended to other supervised learning problems beyond classification with neural networks. For example, in Section 5, we analyze ResMem in a regression setting.

Remark 3.2 (Explicit memorization). Smaller k or σ corresponds to putting higher weight on residuals of the closest neighboring training examples. For sufficiently small k and σ , f_{ResMem} achieves exact memorization of the training sample, i.e., $\text{pred}(f_{\text{ResMem}}(x_i)) = y_i$ for all $i \in [n]$.

3.1 Applicable scenarios of ResMem

We posit that f_{ResMem} yields the largest margin of improvement over f_{DeepNet} when the learning task is “hard” (and thus *implicit* memorization is infeasible). We discuss three such scenarios below. Each of our main empirical or theoretical results roughly corresponds to one of these settings.

- **Hard generalization.** In this scenario, the Bayes-optimal decision boundary is very complex, and is beyond the capability of the neural network itself. To demonstrate this, we analyze a theoretical linear regression problem where the target regression function is not contained in the hypothesis class (cf. Section 5).
- **Hard interpolation.** Here, the number of samples is large enough to make training set interpolation (achieving zero training error) infeasible for a given neural network model. In contrast, ResMem can circumvent the large sample size by explicitly memorizing the training samples. For example, current large language models (LLMs) are typically trained for at most a single epoch over trillions of examples [Chowdhery et al., 2022]. We emulate this scenario by considering a causal language modeling task (cf. Section 4).
- **Efficiency constraint.** In many practical settings, one may prefer a smaller model over a state-of-the-art model due to the training and deployment cost constraints. We emulate such a setting through an image classification task where it is indeed feasible to memorize the training data perfectly using state-of-the-art neural networks, but instead, we use smaller neural networks for computational efficiency (cf. Section 4).

3.2 Relation to existing algorithms

Nearest neighbor method. The nearest neighbor [Cover and Hart, 1967, Knuth, 1973, Hastie et al., 2001, Bottou and Vapnik, 1992] method assigns label to a test sample based on the label of its nearest neighbor(s) in the training set. Owing to its *simplicity*, *flexibility* in defining input similarity, and *computational efficiency* with various approximation schemes [Gionis et al., 1999, Muja and Lowe, 2009], this method remains popular. However, the performance of nearest neighbor drops as data becomes high dimensional [Chaudhuri and Dasgupta, 2014, Muja and Lowe, 2009]. Therefore, to apply it to high dimensional data such as image and text [Zhang et al., 2006], one approach is to learn a representation of data using neural networks [Salakhutdinov and Hinton, 2007]. Following this approach, [Cohen et al., 2018] finds that applying nearest neighbor methods directly to memorize the training labels y_i yields similar performance with the original softmax based neural network classification. In contrast, ResMem applies nearest neighbor to memorize the *residual* r_i of the training samples.

Boosting and residual fitting. Boosting algorithms such as AdaBoost [Freund and Schapire, 1995] seek to construct an ensemble of “weak learner” models with good generalization. AdaBoost achieves this in an iterative manner, and can be interpreted as a particular instantiation of *forward*

stage-wise regression [Friedman et al., 2000], a classical procedure from statistics [Goldberger and Jochems, 1961, Alley, 1987, Tibshirani, 2015]. Intuitively, at each round, one fits the residual of the ensemble of weak learners constructed thus far so as to minimize the exponential loss $\ell_{\text{exp}}(y, f(x)) = e^{-y \cdot f(x)}$. Concretely, for binary classification problems, AdaBoost fits a scorer $f(x) = \sum_{t=1}^T \alpha_t \cdot h_t(x)$, where $\alpha_t \in \mathbb{R}$, $h_t: \mathcal{X} \rightarrow \{\pm 1\}$ is a weak classifier (e.g., a decision stump), and T is the number of rounds of fitting. This fitting is performed iteratively, with (α_t, h_t) learned during the t -th iteration.

Memory-augmented language models. In the language modelling literature, several works explore combining neural models with an external database or memory, which can be queried to retrieve additional context [Lample et al., 2019, Guu et al., 2020, Borgeaud et al., 2021, Li et al., 2022]. Closer to our work, Khandelwal et al. [2020] employ a linear combination of neural network and k -nearest neighbour classifier components. However, our work is quite different in that our k -nearest neighbor components memorizes the *residual* of the DeepNet prediction, whereas Khandelwal et al. [2020] memorizes the target label directly. Various forms of memory have also been considered in generic classification problems [Panigrahy et al., 2021, Vapnik and Izmailov, 2021, Wang and Shao, 2022]. This line of literature again differs from ResMem in that their memory tries to memorize labels directly, whereas ResMem memorizes the *residuals*, leading to a natural combination of the neural network and the memory component.

Model compression for large neural networks. Since ResMem boosts the test accuracy of a small, non-memorizing neural network, we can also view it as a technique that allows a small network to match the performance of a larger one. This relates to the model compression literature. Distillation [Hinton et al., 2015b, Bucilă et al., 2006] is a popular strategy for compressing a large neural model to a smaller one. For a survey of other effective strategies, including pruning, see Menghani [2021]. In Appendix A.2 we discuss that ResMem can be regarded as a “dual procedure” of distillation.

4 Empirical results

In this section, we present three experiments that showcase the efficacy of ResMem. Table 1 provides an overview of our results.

Table 1: Test accuracy for ResMem and baseline deep network.

Dataset	Architecture	Test accuracy	
		DeepNet	ResMem
CIFAR100	CIFAR-ResNet8	56.46%	59.66%
ImageNet	ResNet18	66.86%	67.44%
C4-subset	T5-small	38.01%	40.87%

In Section 4.1, we present the setup for vision (image classification on CIFAR100 and ImageNet) and natural language experiments (autoregressive language modeling). In Section 4.2 we conduct an empirical analysis to explain where the improved accuracy of ResMem comes from. In Section 4.3, we show that ResMem is particularly helpful with large-scale dataset and relatively simple network.

4.1 Experimental setup

CIFAR100. For the CIFAR100 [Krizhevsky, 2009], we use CIFAR-ResNet8 [He et al., 2016] as the base DeepNet. For the DeepNet training, we use SGD with batch size 128, trained for 256 epochs. We use a peak learning rate 0.4, and momentum 0.9. We warm up the learning rate linearly for the first 15 epochs, and decay the learning rate by 0.1 after epochs {96, 192, 224}. For ResMem, we use the pre-logit layer as the image embedding, which has dimension 64. For the nearest neighbor search (Step 3, Section 3), we define the distance between two images to be the ℓ_2 distance between their embeddings. We use $\sigma = 0.7$, $k = 53$, and $T = 1.4$ to compute the weights for the nearest neighbor regressor. We provide the sensitivity analysis of test accuracy against ResMem parameters in Appendix A (cf. Figure 5). We can see that ResMem boosts the test accuracy of CIFAR-ResNet8 from 56.46% to 59.66%, which is between the base DeepNet test accuracy for CIFAR-ResNet8 and CIFAR-ResNet14 (cf. Figure 3(b)).

ImageNet. The experimental setting for ImageNet [Russakovsky et al., 2015] is similar to CIFAR100. We employ a ResNet-18 model [He et al., 2016] and employ the following training procedure. We train the DeepNet for 120 epochs with the batch size of 90. We use an initial learning rate equal 0.8 and an annealing schedule, decreasing the learning rate 10 times after 30, 60 and 80 epochs. We also use warm-up for the first 5 epochs of training, linearly increasing the learning rate from 0.1 up to its initial learning rate. For ResMem, we again use the second last layer of DeepNet as a 512-dimensional embedding of an image and rely on the ℓ_2 distance between the embeddings for nearest neighbor search (Step 3, Section 3). We use $\sigma = 1$, temperature $T = 1$ and $k = 80$ to compute the weights for the nearest neighbor regressor. We provide a similar sensitivity analysis of ResMem hyperparameter for ImageNet in Appendix B.1 (cf. Figure 6). The ResMem improvement on ImageNet is relatively small compared with CIFAR100, since the base ResNet18 test accuracy at 66.86% is already high compared with other base DeepNet accuracies. In addition to the standard ImageNet dataset, we also evaluate ResMem in ImageNet-LT [Liu et al., 2019], a long-tailed version of ImageNet, and observed similar improvement (cf. Appendix B.2).

Natural language experiments For the language experiment, we use a Decoder-Only T5-small [Raffel et al., 2020] model and C4 [Raffel et al., 2020] dataset. C4 is generated from scraping the internet and commonly used as a pretraining dataset or part of the pretraining mix. We pre-trained the DeepNet on C4 training split with auto-regressive language modeling task. For experimental efficiency, we used 1% of the C4 training split (which corresponds to 1,639 million tokens) as the retrieval database, and extracted last transformer layer’s pre-MLP, post-LayerNorm representations as the key embeddings for k NN search, and we created the query embeddings using the whole validation split and the same representation location. For each query, we retrieved 50 neighbors with L_2 distance using ScaNN [Guo et al., 2020]. We used the temperature $T = 1$ for the residual computation and $\sigma = 1$ for computing the neighbor weights. The predicted token is the one with highest probability, similar to greedy decoding, and we measured the prediction accuracy to match the vision experiments. The result in Table 1 shows that ResMem improved test accuracy by 2.86% which is around the accuracy (40.08%) of a T5-base Decoder-Only model trained in a similar way. Please see Appendix C for details on base model training, data processing etc.



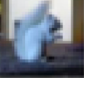
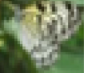

Image classification		Language modeling			
	y^{ResMem}	y^{DeepNet}		y^{ResMem}	y^{DeepNet}
	rose	poppy	...allow for plenty of headroom inside whilst still being less than 2.5m in height.	height	length
	cup	plate	Graphic now consists of all cities with greater than 30,000 locals. Acquiring a home in Spain...	home	residence
	squirrel	rabbit	Filed around 7:30-8:30 a.m. on Friday, March 9, 2012.	March	June
	butterfly	bee	...that will not affect the superior quality of your job. That is possible because we understand how to save...	possible	feasible
	palm tree	pine tree	...answer your questions and schedule the initial meeting. We consistently arrive at the scheduled hour...	consistently	always

Figure 2: Examples from CIFAR100 and C4 test set with the property that (i) y^{ResMem} is correct; (ii) y^{DeepNet} is wrong but close in meaning. We use red to denote the ResMem prediction and blue to denote DeepNet prediction. The DeepNet predictions capture *coarse* structure (e.g., predicting **poppy** for a sample whose true label is **rose**), which can be refined by ResMem capturing the remaining *fine-grained* structure.

4.2 Where does the improvement come from?

In this section, we discuss the accuracy improvement in Table 1. Let $\text{Gain}_{\text{ResMem}}$ be the difference between the test accuracy of ResMem and baseline DeepNet:

$$\text{Gain}_{\text{ResMem}} = L_{01}(f_{\text{ResMem}}) - L_{01}(f_{\text{DeepNet}}),$$

where L_{01} is the misclassification error as defined in equation (1). We offer a decomposition of $\text{Gain}_{\text{ResMem}}$ that sheds light into the mechanism behind ResMem. For a test set $\{(x_i, y_i)\}_{i=1}^m$, let y_i^{ResMem} be the ResMem prediction on instance x_i and let y_i^{DeepNet} be the baseline neural network prediction on x_i . When $y_i^{\text{ResMem}} = y_i^{\text{DeepNet}}$, sample x_i does not contribute to $\text{Gain}_{\text{ResMem}}$. When $y_i^{\text{ResMem}} \neq y_i^{\text{DeepNet}}$, this could arise either from the desirable event where the deep network misclassifies while ResMem classifies correctly; or from the undesirable event where the ResMem misclassifies, while the deep network classifies correctly. These can be summarized by the TPR (*true positive rate*) and FPR (*false positive rate*) respectively:

$$\text{TPR} = \frac{1}{m} \sum_{i=1}^m \mathbb{1}\{y_i^{\text{DeepNet}} \neq y_i \text{ and } y_i^{\text{ResMem}} = y_i\}. \quad (4)$$

$$\text{FPR} = \frac{1}{m} \sum_{i=1}^m \mathbb{1}\{y_i^{\text{DeepNet}} = y_i \text{ and } y_i^{\text{ResMem}} \neq y_i\}. \quad (5)$$

Note that $\text{Gain}_{\text{ResMem}} = \text{TPR} - \text{FPR}$. Table 2 summarizes TPR, FPR, and $\text{Gain}_{\text{ResMem}}$ for the three main experiments discussed in Table 1. The decomposition of $\text{Gain}_{\text{ResMem}}$ says that the gain of ResMem came from the TPR samples, provided they outweigh the FPR samples.

Table 2: True positive rate (TPR) and false positive rate (FPR) for vision and language experiments in Table 1.

Dataset	Architecture	TPR	FPR	Gain _{ResMem}
CIFAR100	ResNet8	5.89%	2.70%	3.19%
ImageNet	ResNet18	3.15%	2.57%	0.58%
C4-subset	T5-small	5.37%	2.44%	2.93%

Analysis of TPR samples Focusing on the test samples where ResMem indeed helps ($y_i^{\text{DeepNet}} \neq y_i$ and $y_i^{\text{ResMem}} = y_i$), we identify a common underlying pattern: while the DeepNet makes an incorrect prediction, it still captures some coarse structure. For example, in the CIFAR100, one sample has correct label $y_i = y_i^{\text{ResMem}} = \text{rose}$, but baseline DeepNet predicts $y_i^{\text{DeepNet}} = \text{poppy}$ (cf. Figure 2). In this case, both **rose** and **poppy** are flowers. We find similar behavior for the language modeling task (cf. Figure 2).

The empirical analysis suggests the DeepNet in isolation can already learn some large scale structures, but is unable to make fine-grained distinctions. This is where ResMem helps: *ResMem helps memorize information in the training label that the DeepNet cannot learn.*

Additional insights from the decomposition. We discuss an alternative way of choosing hyperparameters inspired by the decomposition of $\text{Gain}_{\text{ResMem}}$ into TPR and FPR. In this paper, we choose the ResMem hyperparameters that minimizes the test error on the validation set or, equivalently, maximize $\text{Gain}_{\text{ResMem}}$. With the decomposition of $\text{Gain}_{\text{ResMem}}$, an alternative hyperparameter selection procedure is to use the following optimization problem:

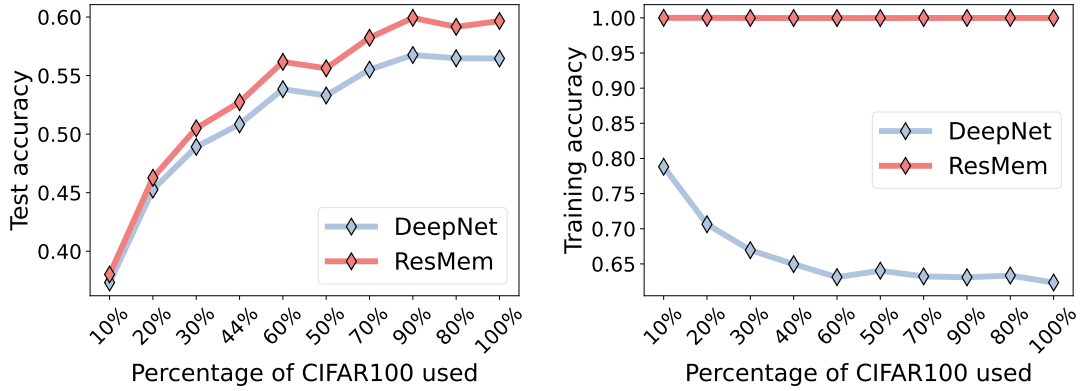
$$\text{maximize}_{\text{FPR}(\text{hyperparam.}) < 0.05} \text{TPR}(\text{hyperparam.}),$$

which ensures that ResMem modifies the predictions of DeepNet in a more conservative manner. In particular, bounding FPR implies that ResMem has minimal impact on the examples where DeepNet already makes correct predictions. At the same time, a higher value of TPR corresponds to maximization of the desirable occurrences where ResMem can correct a wrong prediction by DeepNet.

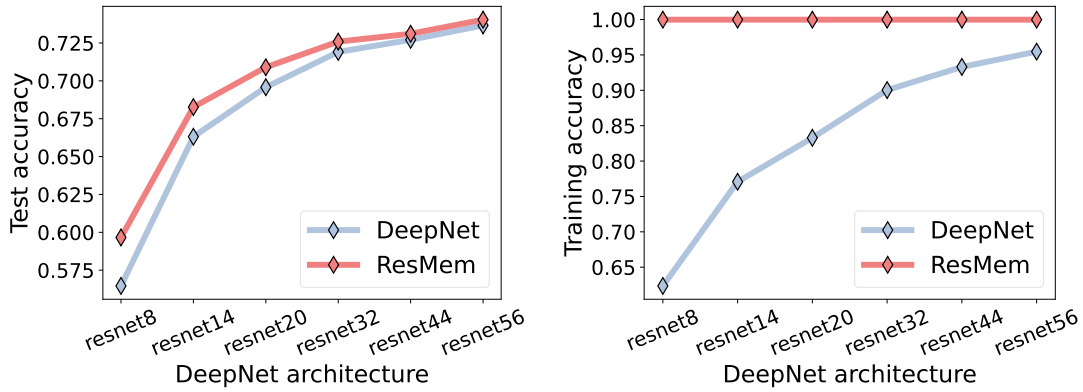
4.3 When does ResMem help?

In this subsection, we present several experiments on CIFAR100 that demonstrates the robustness of the ResMem improvement.

Varying sample size. The main experiment (cf. Table 1) uses the entire CIFAR100 training data. We repeat the experiment with subsets (10%, 20%, ..., 100%) of CIFAR100 training data (subsampling uniformly across different classes). On the left (right) of Figure 3(a), we report the test (training) accuracy of ResMem and baseline DeepNet. As a sanity check, we can see that ResMem always achieves perfect training accuracy, and the DeepNet training accuracy decreases as samples increase (since it’s harder to fit larger dataset). We can see that ResMem yields *progressively larger margin of improvement when more data is used*. This trend suggests a desirable property of ResMem: in real problems where the dataset is extremely large, ResMem is expected to bring even greater benefit.



(a) Test(left)/Training (right) accuracy for different sample sizes.



(b) Test(left)/Training (right) accuracy for different architectures.

Figure 3: Robustness of ResMem improvement with respect to training sample size and deep network architecture. **(a)**: Using 10%, 20%, ..., 100% of training data. **(b)**: Using progressively larger CIFAR-ResNet architecture.

Varying the DeepNet size. We again consider the main CIFAR100 experiment, which was only for a CIFAR-ResNet8 model. We repeat the ResMem evaluation for different models in the CIFAR-ResNet family, i.e., CIFAR-ResNet- $\{8, 14, 20, 32, 44, 56\}$. We use the same choice of training hyperparameter for all six CIFAR-ResNet models, so that only the choice of model architecture changes. DeepNet has progressively better training accuracy as model gets larger, which is intuitive (cf. Figure 3(b)). We find that ResMem yields the *largest margin of improvement when the smallest architecture is applied*, i.e., when it is difficult for the DeepNet itself to interpolate/memorize the data.

5 Theoretical results

As discussed in Section 3, ResMem yields the largest improvement when implicit memorization is infeasible. We provide a concrete result (cf. Theorem 5.3) that characterizes the benefit of ResMem in a stylized linear regression setting.

5.1 Assumptions and setting

In this section, we present the setup and assumptions for the stylized linear regression problem. We consider a setting where the function class that we minimize over does *not* include the ground-truth function that relates the covariates to the response. Therefore, even with infinite samples, the test loss will decay to a positive constant. We exactly characterize the rate of decay, and show that it converges to 0 under ResMem. Our analysis rests on the following assumptions.

Assumption 5.1 (Distribution of covariates). The distribution of covariate $\mathbf{x} \in \mathbb{R}^d$, denoted by $\mathbb{P}_{\mathbf{x}}$, is the uniform distribution over a Euclidean norm ball centered at the origin of radius $\sqrt{d+2}$. The choice of radius ensures that $\mathbb{E}_{\mathbf{x} \sim \mathbb{P}_{\mathbf{x}}} \mathbf{x} \mathbf{x}^\top = \mathbf{I}$.

Assumption 5.2 (Linear regression over norm ball). Consider the problem of learning a linear function $f_\star(\mathbf{x}) = \langle \mathbf{x}, \boldsymbol{\theta}_\star \rangle$ with $\|\boldsymbol{\theta}_\star\| = 1$ from training data $\{(\mathbf{x}_i, y_i)\}_{i=1:n}$ where $\mathbf{x}_i \stackrel{\text{i.i.d.}}{\sim} \mathbb{P}_{\mathbf{x}}$ and $y_i = f_\star(\mathbf{x}_i)$ using the function class

$$\mathcal{F} = \{\mathbf{x} \mapsto \langle \mathbf{x}, \boldsymbol{\theta} \rangle, \|\boldsymbol{\theta}\| < L\}. \quad (6)$$

We assume $L < 1$ so that the problem belongs to the “hard generalization” scenario discussed in Section 3, where the hypothesis space is inadequate to fit the function on its own.

ResMem proceeds by first learning a linear function $f_n(\mathbf{x}) = \langle \boldsymbol{\theta}_n, \mathbf{x} \rangle$ from \mathcal{F} through empirical risk minimization (ERM):

$$\boldsymbol{\theta}_n = \underset{\|\boldsymbol{\theta}\| \leq L}{\operatorname{argmin}} \frac{1}{n} \sum_{i=1}^n [\langle \mathbf{x}_i, \boldsymbol{\theta} \rangle - y_i]^2. \quad (7)$$

The empirical risk minimizer f_n should be thought of as the analog of f_{DeepNet} in the deep learning context. It defines a ground-truth residual function $r_\star(\mathbf{x}) = f_\star(\mathbf{x}) - f_n(\mathbf{x})$. Now we fix a test covariate $\tilde{\mathbf{x}} \sim \mathbb{P}_{\mathbf{x}}$. ResMem “memorizes” the residual function through the 1-nearest neighbor to $\tilde{\mathbf{x}}$

$$r_n(\tilde{\mathbf{x}}) = r_\star(\tilde{\mathbf{x}}_{(1)}) = f_\star(\tilde{\mathbf{x}}_{(1)}) - f_n(\tilde{\mathbf{x}}_{(1)}), \quad (8)$$

where $\tilde{\mathbf{x}}_{(1)}$ is the nearest neighbor to $\tilde{\mathbf{x}}$ among the training covariates $\mathbf{x}_1, \dots, \mathbf{x}_n$:

$$\tilde{\mathbf{x}}_{(1)} = \underset{\mathbf{x} \in \{\mathbf{x}_1, \dots, \mathbf{x}_n\}}{\operatorname{argmin}} \|\mathbf{x} - \tilde{\mathbf{x}}\|.$$

The final prediction is

$$f_n^{\text{ResMem}}(\tilde{\mathbf{x}}) = f_n(\tilde{\mathbf{x}}) + r_n(\tilde{\mathbf{x}}). \quad (9)$$

Observe that if $\tilde{\mathbf{x}}$ coincides with any training sample, $f_n^{\text{ResMem}}(\tilde{\mathbf{x}}) = f_\star(\tilde{\mathbf{x}})$, i.e., we have explicit memorization.

Note that we worked with 1-nearest neighbor regressor for simplicity instead of the general k -nearest neighbor algorithm. The effect of choosing different k is not the main focus of this theoretical analysis.

5.2 A decomposition of the target function

Next, we introduce a decomposition of f_\star , which will help us analyze various components that make up the risk. Define

$$\begin{aligned} \boldsymbol{\theta}_\infty &= \underset{\|\boldsymbol{\theta}\| \leq L}{\operatorname{argmin}} \mathbb{E}_{\mathbf{x} \sim \mathbb{P}_{\mathbf{x}}} [\langle \boldsymbol{\theta}, \mathbf{x} \rangle - \langle \boldsymbol{\theta}_\star, \mathbf{x} \rangle]^2, \\ &= \underset{\|\boldsymbol{\theta}\| \leq L}{\operatorname{argmin}} \|\boldsymbol{\theta} - \boldsymbol{\theta}_\star\| = L\boldsymbol{\theta}_\star, \end{aligned}$$

which is what ERM learns in the limit of $n \rightarrow \infty$. We can think of θ_∞ as the best function that ERM can learn. Then, we can decompose θ_\star into $\theta_\star = \theta_\infty + \theta_\perp$, where $\theta_\perp = \theta_\star - \theta_\infty$. This decomposition can be generalized beyond linear regression. Since θ_∞ defines a function $f_\infty(\mathbf{x}) = \langle \mathbf{x}, \theta_\infty \rangle$, for general non-linear functions, the argument above can be generalized to the decomposition of f_\star to a learnable and non-learnable part

$$f_\star = f_\infty + f_\perp.$$

Intuitively, f_∞ is the best function in \mathcal{F} that ERM can learn, and f_\perp is beyond the capacity of ERM due to the particular choice of function class. ResMem approximates f_\perp using the non-parametric nearest neighbor method.

5.3 A decomposition of the prediction error

We now introduce a decomposition of the prediction risk that reveals how ResMem algorithm boosts generalization. Note that the prediction error of ResMem is

$$\mathbb{E} \left[\left(f_n^{\text{ResMem}}(\tilde{\mathbf{x}}) - f_\star(\tilde{\mathbf{x}}) \right)^2 \right]. \quad (10)$$

It can be decomposed into two components:

$$\begin{aligned} & \mathbb{E} \left[f_n^{\text{ResMem}}(\tilde{\mathbf{x}}) - f_\star(\tilde{\mathbf{x}}) \right]^2 \leq \\ & 3 \times \left[\underbrace{\mathbb{E}(f_n(\tilde{\mathbf{x}}) - f_\infty(\tilde{\mathbf{x}}))^2}_{T_1} + \mathbb{E}(f_n(\tilde{\mathbf{x}}_{(1)}) - f_\infty(\tilde{\mathbf{x}}_{(1)}))^2 + \underbrace{\mathbb{E}(f_\infty(\tilde{\mathbf{x}}) - f_\star(\tilde{\mathbf{x}}) - f_\infty(\tilde{\mathbf{x}}_{(1)}) + f_\star(\tilde{\mathbf{x}}_{(1)}))^2}_{T_2} \right]. \end{aligned}$$

We provide the detail of the decomposition in Section E.1. We can see that T_1 arises due to the difference between f_n and f_∞ (i.e., the estimation error), which, as we will show later, goes to 0 as n goes to infinity:

$$T_1 \rightarrow 0 \text{ as } n \rightarrow \infty.$$

On the other hand, T_2 arises due to the limited capacity of \mathcal{F} . It captures an irreducible error of the risk, which in general is **not** asymptotically zero. However, because of the explicit memorization ResMem algorithm introduces ($\tilde{\mathbf{x}}_{(1)} \rightarrow \tilde{\mathbf{x}}$ as $n \rightarrow \infty$), we also have

$$T_2 \rightarrow 0 \text{ as } n \rightarrow \infty.$$

This decomposition provides a statistical perspective on ResMem: it preserves the asymptotic consistency of T_1 as in classical learning problems while enforcing the asymptotic consistency of T_2 through the nearest-neighbor method.

5.4 Main theoretical result

Given the set up above, we are ready to state the main theoretical result of the paper, which characterizes the rate at which test risk of ResMem approaches 0. The proof of the result below can be found in Appendix E.

Theorem 5.3 (Risk for ResMem algorithm). *For the problem defined in Assumption 5.2 with covariates distribution in Assumption 5.1, the ResMem prediction rule $f_n^{\text{ResMem}}(\tilde{\mathbf{x}})$ defined in equation (9) achieves risk (10)*

$$\mathbb{E} \left[f_n^{\text{ResMem}}(\tilde{\mathbf{x}}) - f_\star(\tilde{\mathbf{x}}) \right]^2 \lesssim d^2 L^2 n^{-2/3} + d^2 (1-L)^2 \left[\frac{\log(n^{1/d})}{n} \right]^{1/d},$$

where \lesssim denotes inequality up to a universal constant independent of d, n and L .

The result includes contribution from two terms introduced in Section 5.3:

- $T_1 \lesssim d^2 L^2 n^{-2/3}$ that arises due to the difference between f_n and f_∞ .
- $T_2 \lesssim [\log(n^{1/d})/n]^{1/d}$ that vanishes as the nearest neighbor of the test point approaches the test point itself $\tilde{\mathbf{x}}_{(1)} \rightarrow \tilde{\mathbf{x}}$.

The two terms T_1 and T_2 can be viewed as “two stages of learning”. Without the ResMem memorization component, we have the usual story of machine learning: $T_1 \rightarrow 0$ at the usual parametric rate, and T_2 stays as an irreducible error, so the overall test error diminishes to a constant at a very fast rate. With the introduction of nearest neighbor memorization procedure, T_2 can also be reduced to 0 at a slower rate, whereas the fast decay of T_1 is still preserved.

This theoretical result shows why it is not favorable to use the k -nearest neighbor component to memorize the response directly: As a corollary of setting $L = 0$ in Theorem 5.3, pure nearest neighbor would result in an overall slow rate of $\approx n^{-1/d}$. However, with ResMem, we can enjoy benefit of having the test loss being asymptotically 0, while also enjoy the fast rate of $n^{-2/3}$ for smaller sample sizes.

6 Discussion and future work

Theoretical results. While Theorem 5.3 shows that ResMem achieves asymptotically zero test risk, another viable strategy is to simply increase the capacity of \mathcal{F} . For example, one may set \mathcal{F} to be a class of suitably wide and deep neural networks, and appeal to standard universal approximation results [Cybenko, 1989]. However, this strategy of scaling the model size comes at the price of increased the training and inference cost. By contrast, ResMem involves augmenting the base predictor with a relatively simple k -nearest neighbor component.

The theory considers the use of the *exact* minimizer θ_n of the empirical risk. For settings involving more complex predictors and losses, (e.g., non-convex neural network objectives), it may be infeasible to obtain this exact minimizer: rather, one obtains an *approximate* minimizer via an iterative optimization procedure, such as SGD. One may augment the analysis to additionally consider the effect of *optimization error* [Bottou and Bousquet, 2007] in such cases. We leave such study for future work.

Empirical procedures. The current formulation of ResMem builds the base DeepNet and k NN components sequentially. Consequently, the DeepNet is trained completely oblivious to the fact that there is a subsequent k NN model that will memorize its residuals. A natural direction of future work is to consider the *joint* training of DeepNet and k NN, so that the models can dynamically interact during training to determine which portion of label is for DeepNet to learn, and the remaining is for k NN to memorize.

A potential problem with applying ResMem to classification is the *mis-calibration* of the scorer. The output of the ResMem prediction vector $f_{\text{ResMem}}(x)$ (3) is not guaranteed to lie on the probability simplex. This is not an issue when we only care about the predicted class membership, since we take the argmax of $f_{\text{ResMem}}(x)$. However, this limitation hinders us to access the *confidence* of the ResMem prediction. To remedy this, a possible future work is to consider alternative notions of residual. For example, we can do memorization in the logit space instead of the probability space. Then, the one-hot encoding of the true label may be replaced by class mean when defining the residual.

Finally, ResMem can be a promising approach to tackle test-time covariate shift. The nearest neighbor modifies the prediction of DeepNet based on the training covariate that are closer to the test covariate, making the algorithm more *adaptive* to the specific test covariate [Sun et al., 2020].

Acknowledgements

Part of the work is done while Zitong Yang is at Google Research, New York. We would like to thank Chong You, Yu Sun, and Yaodong Yu for their feedback on the final draft. Zitong Yang would like to thank Shuangping Li for discussion regarding the proof of Lemma D.1.

References

- William M. Alley. A note on stagewise regression. *The American Statistician*, 41(2):132–134, 1987. doi: 10.1080/00031305.1987.10475461. URL <https://www.tandfonline.com/doi/abs/10.1080/00031305.1987.10475461>.
- Devansh Arpit, Stanisław Jastrzebski, Nicolas Ballas, David Krueger, Emmanuel Bengio, Maxinder S. Kanwal, Tegan Maharaj, Asja Fischer, Aaron Courville, Yoshua Bengio, and Simon Lacoste-Julien. A closer look at memorization in deep networks. In *Proceedings of the 34th International Conference on Machine Learning - Volume 70*, ICML’17, pages 233–242. JMLR.org, 2017.
- Peter L. Bartlett, Dylan J. Foster, and Matus Telgarsky. Spectrally-normalized margin bounds for neural networks. In Isabelle Guyon, Ulrike von Luxburg, Samy Bengio, Hanna M. Wallach, Rob Fergus, S. V. N. Vishwanathan, and Roman Garnett, editors, *Advances in Neural Information Processing Systems 30: Annual Conference on Neural Information Processing Systems 2017, December 4-9, 2017, Long Beach, CA, USA*, pages 6240–6249, 2017.
- Peter L. Bartlett, Philip M. Long, Gábor Lugosi, and Alexander Tsigler. Benign overfitting in linear regression. *Proceedings of the National Academy of Sciences*, 117(48):30063–30070, 2020. doi: 10.1073/pnas.1907378117. URL <https://www.pnas.org/doi/abs/10.1073/pnas.1907378117>.
- Mikhail Belkin, Daniel Hsu, and Partha P. Mitra. Overfitting or perfect fitting? risk bounds for classification and regression rules that interpolate. In *Proceedings of the 32nd International Conference on Neural Information Processing Systems*, NIPS’18, pages 2306–2317, Red Hook, NY, USA, 2018. Curran Associates Inc.
- Sebastian Borgeaud, Arthur Mensch, Jordan Hoffmann, Trevor Cai, Eliza Rutherford, Katie Millican, George van den Driessche, Jean-Baptiste Lespiau, Bogdan Damoc, Aidan Clark, Diego de Las Casas, Aurelia Guy, Jacob Menick, Roman Ring, Tom Hennigan, Saffron Huang, Loren Maggiore, Chris Jones, Albin Cassirer, Andy Brock, Michela Paganini, Geoffrey Irving, Oriol Vinyals, Simon Osindero, Karen Simonyan, Jack W. Rae, Erich Elsen, and Laurent Sifre. Improving language models by retrieving from trillions of tokens. *CoRR*, abs/2112.04426, 2021. URL <https://arxiv.org/abs/2112.04426>.

- Léon Bottou and Olivier Bousquet. The tradeoffs of large scale learning. In J. Platt, D. Koller, Y. Singer, and S. Roweis, editors, *Advances in Neural Information Processing Systems*, volume 20. Curran Associates, Inc., 2007. URL <https://proceedings.neurips.cc/paper/2007/file/0d3180d672e08b4c5312dcdafdf6ef36-Paper.pdf>.
- Léon Bottou and Vladimir Vapnik. Local Learning Algorithms. *Neural Computation*, 4(6): 888–900, 11 1992. ISSN 0899-7667. doi: 10.1162/neco.1992.4.6.888. URL <https://doi.org/10.1162/neco.1992.4.6.888>.
- Alon Brutzkus, Amir Globerson, Eran Malach, and Shai Shalev-Shwartz. SGD learns over-parameterized networks that provably generalize on linearly separable data. In *International Conference on Learning Representations*, 2018. URL <https://openreview.net/forum?id=rJ33wwxRb>.
- Cristian Bucilă, Rich Caruana, and Alexandru Niculescu-Mizil. Model compression. In *Proceedings of the 12th ACM SIGKDD International Conference on Knowledge Discovery and Data Mining*, KDD '06, pages 535–541, New York, NY, USA, 2006. ACM.
- Kamalika Chaudhuri and Sanjoy Dasgupta. Rates of convergence for nearest neighbor classification. In Z. Ghahramani, M. Welling, C. Cortes, N. Lawrence, and K.Q. Weinberger, editors, *Advances in Neural Information Processing Systems*, volume 27. Curran Associates, Inc., 2014. URL <https://proceedings.neurips.cc/paper/2014/file/db957c626a8cd7a27231adfbf51e20eb-Paper.pdf>.
- Chen Cheng, John Duchi, and Rohith Kuditipudi. Memorize to generalize: on the necessity of interpolation in high dimensional linear regression, 2022. URL <https://arxiv.org/abs/2202.09889>.
- Aakanksha Chowdhery, Sharan Narang, Jacob Devlin, Maarten Bosma, Gaurav Mishra, Adam Roberts, Paul Barham, Hyung Won Chung, Charles Sutton, Sebastian Gehrmann, Parker Schuh, Kensen Shi, Sasha Tsvyashchenko, Joshua Maynez, Abhishek Rao, Parker Barnes, Yi Tay, Noam Shazeer, Vinodkumar Prabhakaran, Emily Reif, Nan Du, Ben Hutchinson, Reiner Pope, James Bradbury, Jacob Austin, Michael Isard, Guy Gur-Ari, Pengcheng Yin, Toju Duke, Anselm Levskaya, Sanjay Ghemawat, Sunipa Dev, Henryk Michalewski, Xavier Garcia, Vedant Misra, Kevin Robinson, Liam Fedus, Denny Zhou, Daphne Ippolito, David Luan, Hyeontaek Lim, Barret Zoph, Alexander Spiridonov, Ryan Sepassi, David Dohan, Shivani Agrawal, Mark Omernick, Andrew M. Dai, Thanumalayan Sankaranarayanan Pillai, Marie Pellat, Aitor Lewkowycz, Erica Moreira, Rewon Child, Oleksandr Polozov, Katherine Lee, Zongwei Zhou, Xuezhi Wang, Brennan Saeta, Mark Diaz, Orhan Firat, Michele Catasta, Jason Wei, Kathy Meier-Hellstern, Douglas Eck, Jeff Dean, Slav Petrov, and Noah Fiedel. Palm: Scaling language modeling with pathways, 2022. URL <https://arxiv.org/abs/2204.02311>.
- Gilad Cohen, Guillermo Sapiro, and Raja Giryes. Dnn or k-nn: That is the generalize vs. memorize question, 2018. URL <https://arxiv.org/abs/1805.06822>.
- T. Cover and P. Hart. Nearest neighbor pattern classification. *IEEE Transactions on Information Theory*, 13(1):21–27, 1967. doi: 10.1109/TIT.1967.1053964.
- G Cybenko. Approximation by superpositions of a sigmoidal function. *Mathematics of Control, Signals and Systems*, 2(4):303–314, 1989.

- Gintare Karolina Dziugaite and Daniel M. Roy. Computing nonvacuous generalization bounds for deep (stochastic) neural networks with many more parameters than training data. In *Proceedings of the 33rd Annual Conference on Uncertainty in Artificial Intelligence (UAI)*, 2017.
- Vitaly Feldman. Does learning require memorization? A short tale about a long tail. *CoRR*, abs/1906.05271, 2019. URL <http://arxiv.org/abs/1906.05271>.
- Vitaly Feldman. *Does Learning Require Memorization? A Short Tale about a Long Tail*, page 954–959. Association for Computing Machinery, New York, NY, USA, 2020. ISBN 9781450369794. URL <https://doi.org/10.1145/3357713.3384290>.
- Vitaly Feldman and Chiyuan Zhang. What neural networks memorize and why: Discovering the long tail via influence estimation. In H. Larochelle, M. Ranzato, R. Hadsell, M.F. Balcan, and H. Lin, editors, *Advances in Neural Information Processing Systems*, volume 33, pages 2881–2891. Curran Associates, Inc., 2020a. URL <https://proceedings.neurips.cc/paper/2020/file/1e14bfe2714193e7af5abc64ecbd6b46-Paper.pdf>.
- Vitaly Feldman and Chiyuan Zhang. What neural networks memorize and why: Discovering the long tail via influence estimation. In *Proceedings of the 34th International Conference on Neural Information Processing Systems, NIPS’20*, Red Hook, NY, USA, 2020b. Curran Associates Inc. ISBN 9781713829546.
- Yoav Freund and Robert E. Schapire. A decision-theoretic generalization of on-line learning and an application to boosting. In Paul Vitányi, editor, *Computational Learning Theory*, pages 23–37, Berlin, Heidelberg, 1995. Springer Berlin Heidelberg. ISBN 978-3-540-49195-8.
- Jerome Friedman, Trevor Hastie, and Robert Tibshirani. Additive logistic regression: a statistical view of boosting (With discussion and a rejoinder by the authors). *The Annals of Statistics*, 28(2):337 – 407, 2000. doi: 10.1214/aos/1016218223. URL <https://doi.org/10.1214/aos/1016218223>.
- A. Gionis, Piotr Indyk, and Rajeev Motwani. Similarity search in high dimensions via hashing. In *Very Large Data Bases Conference*, 1999.
- Arthur S. Goldberger and D. B. Jochems. Note on stepwise least squares. *Journal of the American Statistical Association*, 56(293):105–110, 1961. doi: 10.1080/01621459.1961.10482095. URL <https://www.tandfonline.com/doi/abs/10.1080/01621459.1961.10482095>.
- Ruiqi Guo, Philip Sun, Erik Lindgren, Quan Geng, David Simcha, Felix Chern, and Sanjiv Kumar. Accelerating large-scale inference with anisotropic vector quantization. In *International Conference on Machine Learning*, 2020. URL <https://arxiv.org/abs/1908.10396>.
- Kelvin Guu, Kenton Lee, Zora Tung, Panupong Pasupat, and Ming-Wei Chang. Realm: Retrieval-augmented language model pre-training. In *Proceedings of the 37th International Conference on Machine Learning, ICML’20*. JMLR.org, 2020.
- Trevor Hastie, Robert Tibshirani, and Jerome Friedman. *The Elements of Statistical Learning*. Springer Series in Statistics. Springer New York Inc., New York, NY, USA, 2001.
- Kaiming He, Xiangyu Zhang, Shaoqing Ren, and Jian Sun. Deep residual learning for image recognition. In *2016 IEEE Conference on Computer Vision and Pattern Recognition (CVPR)*, pages 770–778, 2016. doi: 10.1109/CVPR.2016.90.

- Geoffrey Hinton, Oriol Vinyals, and Jeff Dean. Distilling the knowledge in a neural network, 2015a. URL <https://arxiv.org/abs/1503.02531>.
- Geoffrey E. Hinton, Oriol Vinyals, and Jeffrey Dean. Distilling the knowledge in a neural network. *CoRR*, abs/1503.02531, 2015b.
- Urvashi Khandelwal, Omer Levy, Dan Jurafsky, Luke Zettlemoyer, and Mike Lewis. Generalization through memorization: Nearest neighbor language models. In *International Conference on Learning Representations*, 2020. URL <https://openreview.net/forum?id=Hk1BjCEkVH>.
- Donald Knuth. *The Art Of Computer Programming, vol. 3: Sorting And Searching*. Addison-Wesley, 1973.
- Alex Krizhevsky. Learning multiple layers of features from tiny images. Technical report, CIFAR, 2009.
- Guillaume Lample, Alexandre Sablayrolles, Marc’Aurelio Ranzato, Ludovic Denoyer, and Hervé Jégou. Large memory layers with product keys. In Hanna M. Wallach, Hugo Larochelle, Alina Beygelzimer, Florence d’Alché-Buc, Emily B. Fox, and Roman Garnett, editors, *Advances in Neural Information Processing Systems 32: Annual Conference on Neural Information Processing Systems 2019, NeurIPS 2019, December 8-14, 2019, Vancouver, BC, Canada*, pages 8546–8557, 2019. URL <https://proceedings.neurips.cc/paper/2019/hash/9d8df73a3cfbf3c5b47bc9b50f214aff-Abstract.html>.
- Zonglin Li, Ruiqi Guo, and Sanjiv Kumar. Decoupled context processing for context augmented language modeling. In Alice H. Oh, Alekh Agarwal, Danielle Belgrave, and Kyunghyun Cho, editors, *Advances in Neural Information Processing Systems*, 2022. URL <https://openreview.net/forum?id=02dbnEbEFn>.
- Tengyuan Liang and Alexander Rakhlin. Just interpolate: Kernel “Ridgeless” regression can generalize. *The Annals of Statistics*, 48(3):1329 – 1347, 2020. doi: 10.1214/19-AOS1849. URL <https://doi.org/10.1214/19-AOS1849>.
- Ziwei Liu, Zhongqi Miao, Xiaohang Zhan, Jiayun Wang, Boqing Gong, and Stella X Yu. Large-scale long-tailed recognition in an open world. In *Proceedings of the IEEE/CVF Conference on Computer Vision and Pattern Recognition*, pages 2537–2546, 2019.
- Gaurav Menghani. Efficient deep learning: A survey on making deep learning models smaller, faster, and better. *CoRR*, abs/2106.08962, 2021. URL <https://arxiv.org/abs/2106.08962>.
- Andrea Montanari and Yiqiao Zhong. The interpolation phase transition in neural networks: Memorization and generalization under lazy training, 2020. URL <https://arxiv.org/abs/2007.12826>.
- Marius Muja and David G. Lowe. Fast approximate nearest neighbors with automatic algorithm configuration. In *International Conference on Computer Vision Theory and Applications*, 2009.
- Behnam Neyshabur, Zhiyuan Li, Srinadh Bhojanapalli, Yann LeCun, and Nathan Srebro. The role of over-parametrization in generalization of neural networks. In *7th International Conference on Learning Representations, ICLR 2019, New Orleans, LA, USA, May 6-9, 2019*. OpenReview.net, 2019.

- Rina Panigrahy, Xin Wang, and Manzil Zaheer. Sketch based memory for neural networks. In Arindam Banerjee and Kenji Fukumizu, editors, *Proceedings of The 24th International Conference on Artificial Intelligence and Statistics*, volume 130 of *Proceedings of Machine Learning Research*, pages 3169–3177. PMLR, 13–15 Apr 2021. URL <https://proceedings.mlr.press/v130/panigrahy21a.html>.
- Colin Raffel, Noam Shazeer, Adam Roberts, Katherine Lee, Sharan Narang, Michael Matena, Yanqi Zhou, Wei Li, and Peter J. Liu. Exploring the limits of transfer learning with a unified text-to-text transformer. *Journal of Machine Learning Research*, 21(140):1–67, 2020. URL <http://jmlr.org/papers/v21/20-074.html>.
- Olga Russakovsky, Jia Deng, Hao Su, Jonathan Krause, Sanjeev Satheesh, Sean Ma, Zhiheng Huang, Andrej Karpathy, Aditya Khosla, Michael Bernstein, Alexander C. Berg, and Li Fei-Fei. ImageNet Large Scale Visual Recognition Challenge. *International Journal of Computer Vision (IJCV)*, 115(3):211–252, 2015. doi: 10.1007/s11263-015-0816-y.
- Ruslan Salakhutdinov and Geoff Hinton. Learning a nonlinear embedding by preserving class neighbourhood structure. In Marina Meila and Xiaotong Shen, editors, *Proceedings of the Eleventh International Conference on Artificial Intelligence and Statistics*, volume 2 of *Proceedings of Machine Learning Research*, pages 412–419, San Juan, Puerto Rico, 21–24 Mar 2007. PMLR. URL <https://proceedings.mlr.press/v2/salakhutdinov07a.html>.
- Yu Sun, Xiaolong Wang, Liu Zhuang, John Miller, Moritz Hardt, and Alexei A. Efros. Test-time training with self-supervision for generalization under distribution shifts. In *ICML*, 2020.
- Ryan J. Tibshirani. A general framework for fast stagewise algorithms. *J. Mach. Learn. Res.*, 16(1):2543–2588, jan 2015. ISSN 1532-4435.
- Vladimir Vapnik and Rauf Izmailov. Reinforced SVM method and memorization mechanisms. *Pattern Recognition*, 119:108018, 2021. ISSN 0031-3203. doi: <https://doi.org/10.1016/j.patcog.2021.108018>. URL <https://www.sciencedirect.com/science/article/pii/S0031320321002053>.
- Martin J Wainwright. *High-dimensional statistics: A non-asymptotic viewpoint*, volume 48. Cambridge University Press, 2019.
- Ke Wang, Vidya Muthukumar, and Christos Thrampoulidis. Benign overfitting in multiclass classification: All roads lead to interpolation, 2021. URL <https://arxiv.org/abs/2106.10865>.
- Zhen Wang and Yuan-Hai Shao. Generalization-memorization machines, 2022. URL <https://arxiv.org/abs/2207.03976>.
- Zitong Yang, Yaodong Yu, Chong You, Jacob Steinhardt, and Yi Ma. Rethinking bias-variance trade-off for generalization of neural networks. In Hal Daumé III and Aarti Singh, editors, *Proceedings of the 37th International Conference on Machine Learning*, volume 119 of *Proceedings of Machine Learning Research*, pages 10767–10777. PMLR, 13–18 Jul 2020. URL <https://proceedings.mlr.press/v119/yang20j.html>.
- Zitong Yang, Yu Bai, and Song Mei. Exact gap between generalization error and uniform convergence in random feature models. In Marina Meila and Tong Zhang, editors, *Proceedings*

of the *38th International Conference on Machine Learning*, volume 139 of *Proceedings of Machine Learning Research*, pages 11704–11715. PMLR, 18–24 Jul 2021. URL <https://proceedings.mlr.press/v139/yang21a.html>.

Chiyuan Zhang, Samy Bengio, Moritz Hardt, Benjamin Recht, and Oriol Vinyals. Understanding deep learning requires rethinking generalization. In *5th International Conference on Learning Representations, ICLR 2017, Toulon, France, April 24-26, 2017, Conference Track Proceedings*. OpenReview.net, 2017.

Hao Zhang, Alexander C. Berg, Michael Maire, and Jitendra Malik. Svm-knn: Discriminative nearest neighbor classification for visual category recognition. In *CVPR (2)*, pages 2126–2136, 2006. URL <https://doi.org/10.1109/CVPR.2006.301>.

A Additional CIFAR100 Results

This section includes additional experiment results on applying ResMem to CIFAR100 dataset.

A.1 Additional robustness results

In addition to the results already presented in Section 4.3, we also evaluate ResMem performance for each architecture in CIFAR-ResNet{8, 14, 20, 32, 44, 56} and each subset (10%, 20%, ..., 100%) of CIFAR100 training data. We use the same training hyperparameter and the ResMem hyperparameter as described in Section 4.1. Generally, we see that ResMem yields larger improvement over the baseline DeepNet when the network is small and dataset is large.

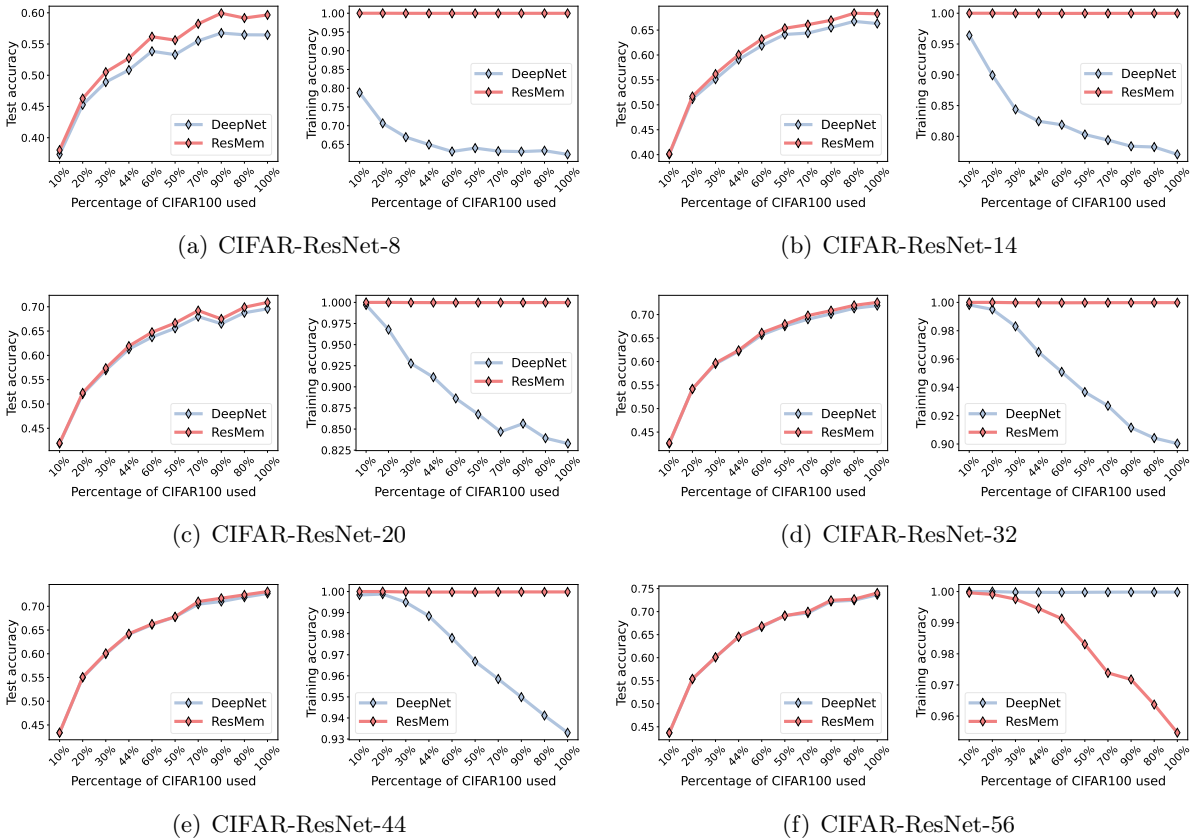


Figure 4: Test(left)/Training (right) accuracy for different sample sizes.

A.2 Sensitivity analysis for CIFAR100

Varying locality parameter k and σ . We vary the number of neighbours from $k = 27$ to $k = 500$. We find that ResMem test accuracy is relatively stable across the choice of the number of neighbours (cf. Figure 5(a)). The trend of the curve suggests that as $k \rightarrow \infty$, the ResMem test accuracy seems to be converging to a constant level. For σ , we explored different values of $\sigma \in (0.1, 2.0)$. We observe that the test accuracy has a unimodal shape as a function of σ , suggesting that there is an optimal choice of σ (cf. Figure 5(b)).

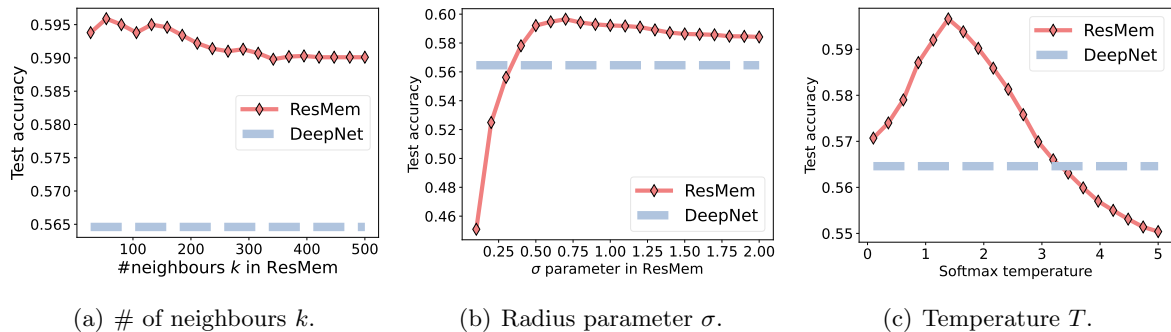


Figure 5: Sensitivity analysis of ResMem hyperparameters. The y -axis represents the CIFAR100 test accuracies, and the x -axis represents the sweeping of respective hyperparameters.

Varying temperature T and connection to distillation. We tried $T = 0.1$ to $T = 5$, and also identified an unimodal shape for the test accuracy (Figure 5(c)). The fact that we can use different temperatures for (a) training the network and (b) constructing the k -NN predictor reminds us of the well-established knowledge distillation procedure [Hinton et al., 2015a]. In knowledge distillation, we first use one model (the teacher network) to generate targets at a higher temperature, and then train a second model (the student network) using the *combination* of the true labels and the output of the first network.

ResMem operates in a reversed direction: Here we have a second model (kNN) that learns the *difference* between true labels and the output of the first model. In both cases, we can tune the temperature of the first model to control how much information is retained. This connection offers an alternative perspective that regards ResMem as a “dual procedure” to knowledge distillation.

B Additional ImageNet results

This section includes additional experiment results on applying ResMem to ImageNet dataset.

B.1 Sensitivity analysis for ImageNet

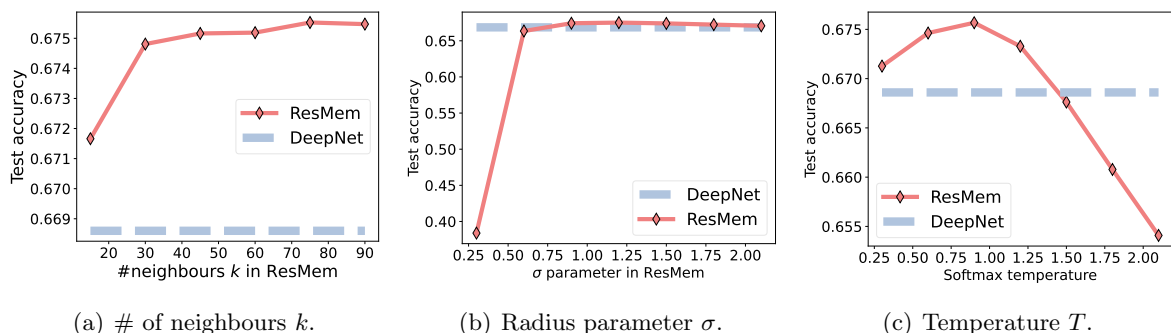


Figure 6: Sensitivity analysis of ResMem hyperparameters. The y -axis represents the imagenet100 test accuracies, and the x -axis represents the sweeping of respective hyperparameters.

We vary the number of neighbours from $k = 15$ to $k = 90$. Similar to CIFAR100 finding, ResMem test accuracy is relatively stable across the choice of the number of neighbours (cf. Figure 6(a)). For σ , we explored different values of $\sigma \in (0.3, 2.1)$. We observe that the test accuracy has a unimodal shape as a function of σ , suggesting that there is an optimal choice of σ (cf. Figure 6(b)). We tried $T = 0.3$ to $T = 2.1$, and also identified an unimodal shape for the test accuracy (Figure 6(c)).

B.2 ImageNet-LT

We also evaluated the proposed ResMem on ImageNet-LT [Liu et al., 2019] – a long-tail version of ImageNet [Russakovsky et al., 2015]. We again utilize ResNet [He et al., 2016] architecture. In particular, we studied the performance of ResMem with both ResNet-18 and ResNet-50 as the underlying DeepNet. We trained the DeepNet for 90 epochs by using SGD with Nesterov momentum. We employ cosine learning rate schedule with the base learning rate of 0.4, and use 0.9 as momentum parameter. Based on a coarse hyperparameter search, we utilized $\sigma = 2.0$ and temperature $T = .8$ in ResMem for both ResNet18 and ResNet50 as the underlying DeepNet. As for the number of neighbors, we utilized $k = 70$ and $k = 90$ for ResNet18 and ResNet50, respectively.

Table 3 showcases the performance of both DeepNet and ResMem on ImageNet-LT. As expected the (balanced) accuracy on ImageNet-LT is worse than that on ImageNet. However, it is also evident from the table that our proposed ResMem leads to performance improvement even in the a large-scale long-tail setting.

Table 3: Test accuracy for ResMem and baseline deep network.

Dataset	Architecture	Test accuracy	
		DeepNet	ResMem
ImageNet	ResNet18	66.86%	67.44%
ImageNet-LT	ResNet18	39.56%	39.91%
ImageNet-LT	ResNet50	46.18%	46.39%

C Additional details of NLP experiments

The Decoder-Only model used in our experiments is essentially the normal Encoder-Decoder architecture with Encoder and Cross-Attention removed. We pretrained both the T5-small and T5-base model on C4 [Raffel et al., 2020] dataset with auto-regressive language modeling task for 1,000,000 steps, with dropout rate of 0.1 and batch size of 128. The learning rate for the first 10,000 steps is fixed to 0.01 and the rest steps follow a square root decay schedule.

During the inference for retrieval key, query embeddings and residuals, we ensured every token has at least 64 preceding context by adopting a sliding window strategy, where a window of 256 token slides from the beginning to the end on each of the articles, with a stride of $256 - 64 = 192$.

For residuals, we only stored the top 128 residuals measured by the absolute magnitude, as the residual vector is as large as T5 vocabulary size (i.e., 32128), and storing all 32128 residuals for each token is too demanding for storage. However, when weight-combining the residuals, we zero filled the missing residuals so that all the residual vectors have 32128 elements.

D Some concentration results for uniform random variables

In this section, we state some concentration results that are useful for the theoretical analysis in Section 5. Let $\tilde{\mathbf{x}}, \mathbf{x}_1, \dots, \mathbf{x}_n \stackrel{\text{i.i.d.}}{\sim} \text{Unif}(\mathcal{B}_{\mathbf{0}, \sqrt{d+2}})$ be i.i.d. samples from the uniform distribution over the Euclidean norm ball of radius $\sqrt{d+2}$ in \mathbb{R}^d . Let

$$Z_n = \min_{\mathbf{x} \in \{\mathbf{x}_1, \mathbf{x}_2, \dots, \mathbf{x}_n\}} \|\tilde{\mathbf{x}} - \mathbf{x}\|^2. \quad (11)$$

If $n = 1$, $\mathbb{E}Z_1$ is the sum of the variance of each coordinate of $\text{Unif}(\mathcal{B}_{\mathbf{0}, \sqrt{d+2}})$. Therefore, $\mathbb{E}Z_n$ provides a generalized measure of concentration. Intuitively, $\mathbb{E}Z_n \rightarrow 0$ as $n \rightarrow \infty$. The proposition below provides an upper bound on the rate of convergence.

Lemma D.1 (Nearest Neighbor concentration). *Given the assumptions above*

$$\mathbb{E}Z_n \lesssim d^2 \left[\frac{\log(n^{1/d})}{n} \right]^{1/d}, \quad (12)$$

where \lesssim means inequality up to an universal constant independent of d and n .

Proof. Define

$$\begin{aligned} \mathcal{E}_1 &= \{Z_n \leq \delta^2\}, \\ \mathcal{E}_2 &= \{\delta \leq \sqrt{d+2} - \|\tilde{\mathbf{x}}\|\}. \end{aligned} \quad (13)$$

We will compute two probabilities $\mathbb{P}(\mathcal{E}_1|\mathcal{E}_2)$ and $\mathbb{P}(\mathcal{E}_2)$ that will be useful later.

$$\begin{aligned} \mathbb{P}(\mathcal{E}_1^c|\mathcal{E}_2) &= \mathbb{P}(Z_n \geq \delta^2|\mathcal{E}_2) = \mathbb{P}(\|\tilde{\mathbf{x}} - \mathbf{x}_i\| \geq \delta, \forall i|\mathcal{E}_2), \\ &= \mathbb{E}_{\tilde{\mathbf{x}}} \mathbb{P}(\|\tilde{\mathbf{x}} - \mathbf{x}_i\| \geq \delta|\mathcal{E}_2, \tilde{\mathbf{x}})^n = \mathbb{E}_{\tilde{\mathbf{x}}} (1 - \mathbb{P}(\|\tilde{\mathbf{x}} - \mathbf{x}_i\| \leq \delta|\mathcal{E}_2, \tilde{\mathbf{x}}))^n, \\ &= \mathbb{E}_{\tilde{\mathbf{x}}} \left[1 - \frac{\text{Vol}(\mathcal{B}_{\tilde{\mathbf{x}}, \delta})}{\text{Vol}(\mathcal{B}_{\mathbf{0}, \sqrt{d+2}})} \right]^n = \left[1 - \left(\frac{\delta}{\sqrt{d+2}} \right)^d \right]^n, \\ &\leq \exp \left[-n \left(\frac{\delta}{\sqrt{d+2}} \right)^d \right]. \end{aligned} \quad (14)$$

Next, we compute $\mathbb{P}(\mathcal{E}_2)$

$$\mathbb{P}(\mathcal{E}_2) = \mathbb{P}(\|\tilde{\mathbf{x}}\| \leq \sqrt{d+2} - \delta) = \left(\frac{\sqrt{d+2} - \delta}{\sqrt{d+2}} \right)^d = \left(1 - \frac{\delta}{\sqrt{d+2}} \right)^d. \quad (15)$$

We use \mathcal{E}_1 and \mathcal{E}_2 to compute the following upper bound

$$\begin{aligned} \mathbb{E}Z_n &= \mathbb{E}(Z_n|\mathcal{E}_1 \cap \mathcal{E}_2)\mathbb{P}(\mathcal{E}_1 \cap \mathcal{E}_2) + \mathbb{E}(Z_n|(\mathcal{E}_1 \cap \mathcal{E}_2)^c)\mathbb{P}((\mathcal{E}_1 \cap \mathcal{E}_2)^c), \\ &\leq \delta^2 + (2\sqrt{d+2})^2 (1 - \mathbb{P}(\mathcal{E}_1 \cap \mathcal{E}_2)), \\ &= \delta^2 + 4(d+2) [1 - \mathbb{P}(\mathcal{E}_1|\mathcal{E}_2)\mathbb{P}(\mathcal{E}_2)]. \end{aligned} \quad (16)$$

To find an upper bound for $\mathbb{E}Z_n$, we need to find an upper bound for $1 - \mathbb{P}(\mathcal{E}_1|\mathcal{E}_2)\mathbb{P}(\mathcal{E}_2)$.

$$\begin{aligned} 1 - \mathbb{P}(\mathcal{E}_1|\mathcal{E}_2)\mathbb{P}(\mathcal{E}_2) &= 1 - [1 - \mathbb{P}(\mathcal{E}_1^c|\mathcal{E}_2)]\mathbb{P}(\mathcal{E}_2), \\ &= 1 - \mathbb{P}(\mathcal{E}_2) + \mathbb{P}(\mathcal{E}_1^c|\mathcal{E}_2)\mathbb{P}(\mathcal{E}_2), \\ &\leq 1 - \mathbb{P}(\mathcal{E}_2) + \mathbb{P}(\mathcal{E}_1^c|\mathcal{E}_2). \end{aligned} \quad (17)$$

Now choose $\delta = \sqrt{d+2}n^{-1/d} [\log(n^{1/d})]^{1/d}$.

$$\mathbb{P}(\mathcal{E}_1^c | \mathcal{E}_2) \leq \exp \left[-n \left(\frac{\delta}{\sqrt{d+2}} \right)^d \right] = \exp \left[-nn^{-1} \log(n^{1/d}) \right] = n^{-1/d}, \quad (18)$$

and

$$\mathbb{P}(\mathcal{E}_2) = \left(1 - \frac{\delta}{\sqrt{d+2}} \right)^d \geq 1 - d \frac{\delta}{\sqrt{d+2}} = 1 - dn^{-1/d} [\log(n^{1/d})]^{1/d}. \quad (19)$$

Thus

$$1 - \mathbb{P}(\mathcal{E}_1 | \mathcal{E}_2) \mathbb{P}(\mathcal{E}_2) \leq 1 - 1 + dn^{-1/d} [\log(n^{1/d})]^{1/d} + n^{-1/d} \lesssim dn^{-1/d} [\log(n^{1/d})]^{1/d}. \quad (20)$$

Combining everything together, we get

$$\begin{aligned} \mathbb{E}Z_n &\leq (d+2)n^{-2/d} [\log(n^{1/d})]^{2/d} + 4(d+2) \times dn^{-1/d} [\log(n^{1/d})]^{1/d}, \\ &\lesssim d^2 n^{-1/d} [\log(n^{1/d})]^{1/d}, \\ &= d^2 \left[\frac{\log(n^{1/d})}{n} \right]^{1/d}. \end{aligned} \quad (21)$$

This completes the proof. \square

Proposition D.2 (Wainwright [2019] Corollary 6.20). *Let $\mathbf{x}_i \stackrel{\text{i.i.d.}}{\sim} \text{Unif}(\mathcal{B}_{\mathbf{0}, \sqrt{d+2}})$ for $i = 1, \dots, n$ be uniformly distributed over a ball of radius B in \mathbb{R}^d centered at $\mathbf{0}$. Let*

$$\boldsymbol{\Sigma}_n = \frac{1}{n} \sum_{i=1}^n \mathbf{x}_i \mathbf{x}_i^\top$$

be the sample covariance matrix. Then

$$\mathbb{P}(\|\boldsymbol{\Sigma}_n - \mathbf{I}\|_{\text{op}} > \varepsilon) \leq 2d \exp \left[-\frac{n\varepsilon^2}{2(d+2)(1+\varepsilon)} \right].$$

E Proof of Theorem 5.3

In this section, we present the proof of Theorem 5.3. In Section E.1, we provide the detail of the decomposition of the risk into T_1 and T_2 . Then in Section E.2 we compute an upper bound for T_1 , and compute an upper bound for T_2 in Section E.3. Finally, we combine everything together in Section E.4 and completes the proof.

E.1 Decomposition of the test risk

$$\begin{aligned}
& \mathbb{E} \left[f^{\text{ResMem}}(\tilde{\mathbf{x}}) - f_*(\tilde{\mathbf{x}}) \right]^2 = \mathbb{E} [f_n(\tilde{\mathbf{x}}) + r_n(\tilde{\mathbf{x}}) - f_*(\tilde{\mathbf{x}})]^2, \\
& = \mathbb{E} [f_n(\tilde{\mathbf{x}}) - f_*(\tilde{\mathbf{x}}) - f_n(\tilde{\mathbf{x}}_{(1)}) + f_*(\tilde{\mathbf{x}}_{(1)})]^2, \\
& = \mathbb{E} [f_n(\tilde{\mathbf{x}}) - f_\infty(\tilde{\mathbf{x}}) + f_\infty(\tilde{\mathbf{x}}) - f_*(\tilde{\mathbf{x}}) - f_n(\tilde{\mathbf{x}}_{(1)}) + f_\infty(\tilde{\mathbf{x}}_{(1)}) - f_\infty(\tilde{\mathbf{x}}_{(1)}) + f_*(\tilde{\mathbf{x}}_{(1)})]^2, \\
& \leq 3 \times \underbrace{\mathbb{E}(f_n(\tilde{\mathbf{x}}) - f_\infty(\tilde{\mathbf{x}}))^2}_{T_1} + \underbrace{\mathbb{E}(f_n(\tilde{\mathbf{x}}_{(1)}) - f_\infty(\tilde{\mathbf{x}}_{(1)}))^2 + \mathbb{E}(f_\infty(\tilde{\mathbf{x}}) - f_*(\tilde{\mathbf{x}}) - f_\infty(\tilde{\mathbf{x}}_{(1)}) + f_*(\tilde{\mathbf{x}}_{(1)}))^2}_{T_2},
\end{aligned} \tag{22}$$

where in the last inequality, we used the fact that $(a + b + c)^2 < 3(a^2 + b^2 + c^2)$ for any $a, b, c \in \mathbb{R}$.

E.2 Upper bound on T_1 .

Since $\mathbb{P}_{\mathbf{x}} = \text{Unif}(\mathcal{B}_{0,B})$, we apply the bound $\|\tilde{\mathbf{x}}\|, \|\tilde{\mathbf{x}}_{(1)}\| \leq B$ to obtain

$$\begin{aligned}
T_1 & = \mathbb{E}[f_n(\tilde{\mathbf{x}}) - f_\infty(\tilde{\mathbf{x}})]^2 + \mathbb{E}[f_n(\tilde{\mathbf{x}}_{(1)}) - f_\infty(\tilde{\mathbf{x}}_{(1)})]^2, \\
& = \mathbb{E}\langle \boldsymbol{\theta}_n - \boldsymbol{\theta}_\infty, \tilde{\mathbf{x}} \rangle^2 + \mathbb{E}\langle \boldsymbol{\theta}_n - \boldsymbol{\theta}_\infty, \tilde{\mathbf{x}}_{(1)} \rangle^2, \\
& \leq \mathbb{E}\|\boldsymbol{\theta}_n - \boldsymbol{\theta}_\infty\|^2 \|\tilde{\mathbf{x}}\|^2 + \mathbb{E}\|\boldsymbol{\theta}_n - \boldsymbol{\theta}_\infty\|^2 \|\tilde{\mathbf{x}}_{(1)}\|^2, \\
& \leq 2B^2 \mathbb{E}\|\boldsymbol{\theta}_n - \boldsymbol{\theta}_\infty\|^2.
\end{aligned} \tag{23}$$

As n gets large, the empirical covariance matrix $\boldsymbol{\Sigma}_n = \mathbf{X}^\top \mathbf{X}/n$ is concentrated around its mean \mathbf{I} . Let $\boldsymbol{\Delta}_n = \mathbf{I} - \boldsymbol{\Sigma}_n$ denote this deviation. For some $\varepsilon \in (0, 1)$, define the following ‘‘good event’’ over the randomness in $\boldsymbol{\Sigma}_n$

$$\mathcal{A} = \{\|\boldsymbol{\Delta}_n\|_{\text{op}} < \varepsilon\}, \tag{24}$$

where $\|\boldsymbol{\Delta}_n\|_{\text{op}}$ denotes the operator norm of the deviation matrix. The high level idea of the proof is to condition on the event \mathcal{A} and deduce an upper bound of $\|\boldsymbol{\theta}_n - \boldsymbol{\theta}_\infty\|$ in terms of ε . Then, we use the fact that \mathcal{A} happens with high probability.

Recall that $\boldsymbol{\theta}_\infty = L\boldsymbol{\theta}_*$, and

$$\boldsymbol{\theta}_n = \underset{\|\boldsymbol{\theta}\| \leq L}{\text{argmin}} \frac{1}{n} \|\mathbf{X}\boldsymbol{\theta} - \mathbf{y}\|^2. \tag{25}$$

Since $\mathbf{y} = \mathbf{X}\boldsymbol{\theta}_*$ by definition, the Lagrangian of the convex program above is

$$\mathcal{L}(\boldsymbol{\theta}, \lambda) = \frac{1}{n} \|\mathbf{X}\boldsymbol{\theta} - \mathbf{X}\boldsymbol{\theta}_*\|^2 + \lambda(\|\boldsymbol{\theta}\|^2 - L). \tag{26}$$

The KKT condition suggests that the primal-dual optimal pair $(\boldsymbol{\theta}_n, \lambda_n)$ is given by

$$\begin{aligned}
\|\boldsymbol{\theta}_n\| & \leq L, \\
\lambda_n & \geq 0, \\
\lambda_n(\|\boldsymbol{\theta}_n\| - L) & = 0,
\end{aligned} \tag{27}$$

and at optimality

$$\begin{aligned}\nabla_{\boldsymbol{\theta}} \mathcal{L}(\boldsymbol{\theta}_n, \lambda_n) = 0 &\iff \frac{2}{n} \mathbf{X}^\top \mathbf{X}(\boldsymbol{\theta} - \boldsymbol{\theta}_*) + 2\lambda_n \boldsymbol{\theta} = 0, \\ &\iff \boldsymbol{\theta}_n = (\boldsymbol{\Sigma}_n + \lambda_n \mathbf{I})^{-1} \boldsymbol{\Sigma}_n \boldsymbol{\theta}_*.\end{aligned}\tag{28}$$

The complementary slackness condition $\lambda_n(\|\boldsymbol{\theta}_n\| - L) = 0$ suggests that either $\lambda_n = 0$ or $\|\boldsymbol{\theta}_n\| = L$. But if $\lambda_n = 0$, the stationary condition $\nabla_{\boldsymbol{\theta}} \mathcal{L}(\boldsymbol{\theta}, \lambda) = 0$ would suggest that $\boldsymbol{\theta}_n = \boldsymbol{\Sigma}_n^{-1} \boldsymbol{\Sigma}_n \boldsymbol{\theta}_* = \boldsymbol{\theta}_* \Rightarrow \|\boldsymbol{\theta}_n\| = 1 > L$, a contradiction. (Note that here $\boldsymbol{\Sigma}_n$ is invertible condition on the event \mathcal{A} .) Therefore, we must have $\|\boldsymbol{\theta}_n\| = L$. As a result, the primal and dual pair $(\boldsymbol{\theta}_n, \lambda_n)$ is determined by the system of equations

$$\begin{cases} \boldsymbol{\theta}_n &= (\boldsymbol{\Sigma}_n + \lambda_n \mathbf{I})^{-1} \boldsymbol{\Sigma}_n \boldsymbol{\theta}_*, \\ \|\boldsymbol{\theta}_n\| &= L, \\ \lambda_n &> 0. \end{cases}\tag{29}$$

Next, we proceed to compute the deviation $\|\boldsymbol{\theta}_n - \boldsymbol{\theta}_\infty\|$.

$$\begin{aligned}\boldsymbol{\theta}_n &= [(\lambda_n + 1)\mathbf{I} - \boldsymbol{\Delta}_n]^{-1} \boldsymbol{\Sigma}_n \boldsymbol{\theta}_*, \\ &= (\lambda_n + 1)^{-1} \left[\mathbf{I} - \frac{\boldsymbol{\Delta}_n}{\lambda_n + 1} \right]^{-1} \boldsymbol{\Sigma}_n \boldsymbol{\theta}_*, \\ &= (\lambda_n + 1)^{-1} \left[\mathbf{I} + \sum_{k=1}^{\infty} \frac{\boldsymbol{\Delta}_n^k}{(\lambda_n + 1)^k} \right] (\mathbf{I} - \boldsymbol{\Delta}_n) \boldsymbol{\theta}_*, \\ &= (\lambda_n + 1)^{-1} \left[\mathbf{I} + \sum_{k=1}^{\infty} \frac{\boldsymbol{\Delta}_n^k}{(\lambda_n + 1)^k} - \boldsymbol{\Delta}_n - \sum_{k=1}^{\infty} \frac{\boldsymbol{\Delta}_n^{k+1}}{(\lambda_n + 1)^k} \right] \boldsymbol{\theta}_*, \\ &= (\lambda_n + 1)^{-1} \boldsymbol{\theta}_* + (\lambda_n + 1)^{-1} \boldsymbol{\Delta}_n \left[\sum_{k=1}^{\infty} \frac{\boldsymbol{\Delta}_n^{k-1}}{(\lambda_n + 1)^k} - \mathbf{I} - \sum_{k=1}^{\infty} \frac{\boldsymbol{\Delta}_n^k}{(\lambda_n + 1)^k} \right] \boldsymbol{\theta}_*, \\ &= (\lambda_n + 1)^{-1} \boldsymbol{\theta}_* + (\lambda_n + 1)^{-1} \boldsymbol{\Delta}_n \left[\sum_{k=1}^{\infty} \frac{\boldsymbol{\Delta}_n^{k-1} - \boldsymbol{\Delta}_n^k}{(\lambda_n + 1)^k} - \mathbf{I} \right] \boldsymbol{\theta}_*.\end{aligned}\tag{30}$$

Define

$$\mathbf{D}_n = \boldsymbol{\Delta}_n \left[\sum_{k=1}^{\infty} \frac{\boldsymbol{\Delta}_n^{k-1} - \boldsymbol{\Delta}_n^k}{(\lambda_n + 1)^k} - \mathbf{I} \right].\tag{31}$$

Then $\boldsymbol{\theta}_n = (\lambda_n + 1)^{-1} \boldsymbol{\theta}_* + (\lambda_n + 1)^{-1} \mathbf{D}_n \boldsymbol{\theta}_*$, and

$$\begin{aligned}\|\mathbf{D}_n\| &\leq \|\boldsymbol{\Delta}_n\| \left[1 + \sum_{k=1}^{\infty} \frac{\|\boldsymbol{\Delta}_n\|^{k-1} + \|\boldsymbol{\Delta}_n\|^k}{(\lambda_n + 1)^k} \right], \\ &\leq \varepsilon \left[1 + 2(1 + \lambda_n)^{-1} \sum_{k=1}^{\infty} \left(\frac{\varepsilon}{1 + \lambda_n} \right)^k \right], \\ &= \varepsilon \left(1 + \frac{2}{1 + \lambda_n} \frac{1}{1 - \frac{\varepsilon}{1 + \lambda_n}} \right) \leq 3\varepsilon.\end{aligned}\tag{32}$$

Therefore

$$\begin{aligned} L &= \|\boldsymbol{\theta}_n\|^2 = (\lambda_n + 1)^{-2} + (\lambda_n + 1)^{-2} \boldsymbol{\theta}_*^\top \mathbf{D}_n^\top \mathbf{D}_n \boldsymbol{\theta}_* + 2(\lambda_n + 1)^{-2} \boldsymbol{\theta}_*^\top \mathbf{D}_n \boldsymbol{\theta}_*, \\ \Rightarrow (\lambda_n + 1)^2 L^2 &= 1 + \delta_n, \quad \delta_n = \boldsymbol{\theta}_*^\top \mathbf{D}_n^\top \mathbf{D}_n \boldsymbol{\theta}_* + 2\boldsymbol{\theta}_*^\top \mathbf{D}_n \boldsymbol{\theta}_*. \end{aligned} \quad (33)$$

We can obtain the following bound for δ_n :

$$|\delta_n| \leq \|\boldsymbol{\theta}_*\|^2 \|\mathbf{D}_n\|^2 + 2\|\boldsymbol{\theta}_*\| \|\mathbf{D}_n\| \leq 9\varepsilon^2 + 6\varepsilon \leq 15\varepsilon. \quad (34)$$

Since $1 - \delta_n/2 \leq \sqrt{1 + \delta_n} \leq 1 + \delta_n/2$, and $|\delta_n| \leq 15\varepsilon$, we obtain

$$|(\lambda_n + 1)L - 1| \leq \frac{15\varepsilon}{2} \Rightarrow |L - (\lambda_n + 1)^{-1}| \leq \frac{15\varepsilon}{2} (\lambda_n + 1)^{-1} \leq \frac{15\varepsilon}{2}, \quad (35)$$

where the last inequality follows as we have $\lambda_n > 0$. Finally,

$$\begin{aligned} \boldsymbol{\theta}_n - \boldsymbol{\theta}_\infty &= (\lambda_n + 1)^{-1} \boldsymbol{\theta}_* - L\boldsymbol{\theta}_* + (\lambda_n + 1)^{-1} \mathbf{D}_n \boldsymbol{\theta}_*, \\ \Rightarrow \|\boldsymbol{\theta}_n - \boldsymbol{\theta}_\infty\|^2 &= [(1 + \lambda_n)^{-1} - L]^2 + (1 + \lambda_n)^{-2} \boldsymbol{\theta}_*^\top \mathbf{D}_n^\top \mathbf{D}_n \boldsymbol{\theta}_* + 2(\lambda_n + 1)^{-1} [(1 + \lambda_n)^{-1} - L] \boldsymbol{\theta}_*^\top \mathbf{D}_n \boldsymbol{\theta}_*, \\ &\leq 64\varepsilon^2 + 9\varepsilon^2 + 45\varepsilon^2 = 118\varepsilon^2, \\ \Rightarrow \|\boldsymbol{\theta}_n - \boldsymbol{\theta}_\infty\|^2 &\lesssim \varepsilon^2. \end{aligned} \quad (36)$$

Combine the above result with Proposition D.2, we get that

$$\begin{aligned} \mathbb{E}\|\boldsymbol{\theta}_n - \boldsymbol{\theta}_\infty\|^2 &= \mathbb{E}(\|\boldsymbol{\theta}_n - \boldsymbol{\theta}_\infty\|^2 | \mathcal{A}) \mathbb{P}(\mathcal{A}) + \mathbb{E}(\|\boldsymbol{\theta}_n - \boldsymbol{\theta}_\infty\|^2 | \mathcal{A}^c) \mathbb{P}(\mathcal{A}^c), \\ &\leq \varepsilon^2 + 4L^2 \times 4d \exp\left[-\frac{n\varepsilon^2}{2(d+2)(1+\varepsilon)}\right], \end{aligned} \quad (37)$$

If we choose $\varepsilon = n^{-1/3}$, we get

$$\mathbb{E}\|\boldsymbol{\theta}_n - \boldsymbol{\theta}_\infty\|^2 \lesssim dL^2 n^{-2/3}, \quad (38)$$

which implies that

$$T_1 \lesssim d^2 L^2 n^{-2/3}. \quad (39)$$

E.3 Upper bound on T_2 .

Plugging in the formula for $f_\perp(\tilde{\mathbf{x}}) = f_*(\tilde{\mathbf{x}}) - f_\infty(\tilde{\mathbf{x}}) = \langle \tilde{\mathbf{x}}, \boldsymbol{\theta}_\perp \rangle$, we get

$$\begin{aligned} T_2 &= \mathbb{E}[f_\perp(\tilde{\mathbf{x}}_{(1)}) - f_\perp(\tilde{\mathbf{x}})]^2, \\ &= \mathbb{E}\langle \boldsymbol{\theta}_\perp, \tilde{\mathbf{x}}_{(1)} - \tilde{\mathbf{x}} \rangle^2, \\ &\leq (1 - L)^2 \|\boldsymbol{\theta}_*\|^2 \mathbb{E}\|\tilde{\mathbf{x}} - \tilde{\mathbf{x}}_{(1)}\|^2, \\ &= (1 - L)^2 \mathbb{E}\|\tilde{\mathbf{x}} - \tilde{\mathbf{x}}_{(1)}\|^2, \end{aligned} \quad (40)$$

where in the last inequality, we used the relation that $\boldsymbol{\theta}_\perp = (1 - L)\boldsymbol{\theta}_*$. Proposition D.1 suggests that

$$\mathbb{E}\|\tilde{\mathbf{x}} - \tilde{\mathbf{x}}_{(1)}\|^2 \lesssim d^2 \left[\frac{\log(n^{1/d})}{n} \right]^{1/d}, \quad (41)$$

which implies

$$T_2 \lesssim d^2 (1 - L)^2 \left[\frac{\log(n^{1/d})}{n} \right]^{1/d}. \quad (42)$$

Remark E.1 (Comparison with pure nearest neighbor and ERM). If we rely solely on nearest neighbor method, the prediction error is

$$\mathbb{E}[f_\star(\tilde{\mathbf{x}}) - f_\star(\tilde{\mathbf{x}}_{(1)})]^2 = \mathbb{E}\langle \tilde{\mathbf{x}} - \tilde{\mathbf{x}}_{(1)}, \boldsymbol{\theta}_\star \rangle^2 \leq \mathbb{E}\|\tilde{\mathbf{x}} - \tilde{\mathbf{x}}_{(1)}\|^2. \quad (43)$$

On the other hand, if we solely rely on ERM, even with infinite sample, we get

$$\mathbb{E}[f_\star(\tilde{\mathbf{x}}) - f_\infty(\tilde{\mathbf{x}})]^2 = \mathbb{E}\langle \tilde{\mathbf{x}}, \boldsymbol{\theta}_\star - \boldsymbol{\theta}_\infty \rangle^2 \leq (1 - L)^2 \mathbb{E}\|\tilde{\mathbf{x}}\|^2. \quad (44)$$

We can see from the upper bound that ResMem takes advantage of both

- Projecting f_\star onto f_∞ , so that the dependence on the prediction function is reduced from 1 to $(1 - L)^2$.
- Memorizing the residuals using nearest neighbor, so that the variance is reduced from $\mathbb{E}\|\tilde{\mathbf{x}}\|^2$ to $\mathbb{E}\|\tilde{\mathbf{x}}_{(1)} - \tilde{\mathbf{x}}\|^2$.

E.4 Test loss for ResMem.

If we combine the previous two parts together, we get

$$\mathbb{E}\left[\hat{f}(\tilde{\mathbf{x}}) - f_\star(\tilde{\mathbf{x}})\right]^2 \lesssim d^2 L^2 n^{-2/3} + d^2 (1 - L)^2 \left[\frac{\log(n^{1/d})}{n}\right]^{1/d}. \quad (45)$$

This completes the proof of Theorem 5.3.